The object of this researching is the process of maneuvering a sea-based vehicle under compressed conditions, which requires one hundred percent reserve of thrusters (THRs) of various modifications and locations. The main problem is the provision of energy-efficient control over the ship's motion at low speed in the horizontal plane using a high-level predictive controller. The hierarchy of the motion control system (MCS) is usually divided into several levels with the help of a high-level motion controller and the THR motor control distribution algorithm. This allows for a modular software structure where a high-level controller (HLC) can be designed without using comprehensive information about the THR motors. However, for a certain reference of THR configurations, such a decoupling can lead to reduced control performance due to the limitations of HLC regarding the physical constraints of the vessel and the behavior of MCS.

The main results of the researching are methods to improve control performance using a nonlinear model predictive control (MPC) as a basis for the designed motion controllers due to its optimized solution and ability to consider constraints. A decoupled system was implemented for two simple motor tasks showing dissociation problems. The shortcomings were eliminated through the development of a nonlinear MPC controller, which combines the motion controller and the distribution of control over THR motors. To preserve the discrete modularity of the control system and achieve adequate performance, a nonlinear MPC controller with time-varying constraints was designed. This has made it possible to take into account the current limitations of the THR control system, increase the accuracy of control, and reduce the response time of the system by 10 %

Keywords: propulsion system, predictive control, distributed system, high-level controller

UDC 629.56
DOI: 10.15587/1729-4061.2024.313627

DESIGN OF THE PREDICTIVE MANAGEMENT AND CONTROL SYSTEM FOR COMBINED PROPULSION COMPLEX

Vitalii Budashko
Doctor of Technical Sciences, Professor
Department of Electrical Engineering and Electronics*
Albert Sandler
Corresponding author
PhD, Associate Professor
Department of the theory of automatic control and computer technology*
E-mail: albertsand4@gmail.com
Sergii Khniunin
PhD, Associate Professor*
Valentyn Bogach
PhD, Associate Professor
Department of Materials Technology and Ship Repair
Educational and Scientific Institute of of Engineering**
*Educational and Scientific Institute of Automation and Electromechanics**
**National University "Odessa Maritime Academy"
Didrikhson str., 8, Odesa, Ukraine, 65052

Received date 16.07.2024
Accepted date 30.09.2024
Published date 30.10.2024

***How to Cite**: Budashko, V., Sandler, A., Khniunin, S., Bogach, V. (2024). Design of the predictive management and control system for combined propulsion complex. Eastern-European Journal of Enterprise Technologies, 5 (2 (131)), 90–102. https://doi.org/10.15587/1729-4061.2024.313627*

1. Introduction

The methodology of applying nonlinear model predictive control (MPC) is increasingly used as a basis in motion control systems of combined propulsion systems (CPS) of marine vessels with propulsion devices.

The main aspects of the state-of-the-art development of nonlinear predictive control include:

– relevant case studies and working examples that demonstrate methods to apply modeling and design management regarding proprietary projects;

– a GitHub repository with MATLAB scripts and a relevant toolset, compatible with the latest versions of MathWorks software;

– new content of mathematical modeling, including models for ships and underwater vehicles, hydrodynamics, control forces and moments;

– new methods of orientation and navigation, including the line of sight (LOS) laws, sensor systems, model-based navigation systems, and inertial navigation systems.

Ships working under THR's mode use the largest number of THRs to maintain position, which leads to overloading of the ship's electrical power system or its inefficient use. This happens on the one hand, as a result of ensuring accurate positioning, and on the other hand, due to excessive power reserve in case of failure of one or more THRs.

Expanding the scope of conventional DP systems, for example to include automated mooring and docking for tankers or low speed passenger ferries, these systems need to be adapted for the new list of vessels. These vessels are generally designed without redundant power equipment and may not be as maneuverable as THR-capable vessels. This means that the control system must make better use of the available energy efficiency, providing both a higher level of automation for a wide range of vessels and an increase in the energy efficiency of the vessel with a DP system.

The main remaining problem is the provision of energy-efficient control over the ship's motion at low speed in the horizontal plane using a high-level predictive control controller. Therefore, studies aimed at designing predictive control systems are relevant.

2. Literature review and problem statement

Works [1, 2] report the results of the latest research in the field of hydrodynamics, navigation, and control systems of sea vessels. In [1], the authors prove how the implementation of mathematical models and modern management theory could be used for modeling and verification of control systems, decision support systems, and situational identification systems. Current case studies and working examples of the application of control system modeling methods are given in [2]. However, in these works, the authors had difficulties in devising scenarios for managing distributed subsystems compatible with the latest versions of software from MathWorks.

Research that includes hydrodynamic models for sea vessels, wind, waves, and ocean currents can be an option to overcome these difficulties [3]. But, taking into account the dynamics and stability of sea vessels, expanding the principles of dynamic positioning, synthesis and identification of sensors and aspects of inertial navigation remain relevant.

In work [4], the authors tried to apply the latest tools for the analysis and design of advanced guidance, navigation, and control (GNC) systems using the example of control over unmanned underwater, surface, and autonomous vehicles. However, the reported examples of engineering developments do not give reason to believe that MATLAB scenarios for practical implementation and software testing are perfect.

For example, one of the most problematic systems today are dynamic positioning systems (DP) [5]. DP systems are used to hold a vessel or rig stationary in a horizontal plane or to move at a low constant speed using only available thrusters (THRs). The main criterion for the efficiency of using DP systems is the criterion of minimum fuel consumption with minimum wear of the power plant [6]. But, making the control task simpler by reducing the DP problem to compensation in three degrees of freedom of the horizontal plane using (three) independent PID controllers is possible only under favorable conditions.

The first condition is the expansion of the working space in which the designed controllers work, through the application of algorithms of the Low Speed Motion Control method [7–9]. In [7], the authors managed to devise a method of sensorless control based on tracking the behavior of the control object with the implementation of a high-frequency control signal in the process of its demodulation. The achievement of optimal control is implemented in real time according to the principle of predictive control, which provides almost optimal control over the vessel and THR, but without taking into account the possibility of changing the boundary conditions.

Sensorless control algorithms were improved in [8]. Through the use of a stochastic neurofuzzy system of disturbances based on the algorithmization of the work of the constituent swarms with the use of iterative learning, a method for combining the learning results during the current error analysis was proposed. The performance of the controller was also checked using the method of comparison with other software computation methods.

In [9], the authors managed to introduce a high-frequency sinusoidal signal of the supply voltage of THR to the calculated axis of the synchronous rotating coordinate system and obtain an estimation error containing information about the rotor position. By detecting the output signal of the PI controller of the current circuit of the quadrature axis, it became possible to estimate the initial position of the rotor and the magnetic field of the stator. It was proposed to implement the determination of the actual position of the rotor by the method of non-positional static control. But, according to the simulation results, this method did not make it possible to accurately determine the position and speed of the motor rotor both at zero and at low speed.

The algorithmic structure shown in Fig. 4 [10] is common to many automated vessels. The highest level Motion Control System (MCS) calculates the total forces and moments that must be applied to the vessel. Algorithm distribution or THR's location matrix calculates the reference value of the orientation and speed of the propellers for the individual motors to obtain the forces that are specified by the motion controller. This method is known as decoupled control [11]. The decoupling provides a more flexible and modular design, as the high-level controller setup can remain the same for vessels with different THR's configurations, while only the thrust values for THRs are updated for the new configuration. However, this can also be an important drawback. For example, the development of closed-loop control algorithms requires that the high-level motion controller does not take into account the physical limitations of the ship and THR motors [12]. This can create a problem with the overall energy efficiency of the control system.

The MPC controller design technology is based on using the MATLAB interface for the open-source ACADO (Automatic Control and Dynamic Optimization) toolkit [13] with the optimization problem solved in [14]. Code was generated for the online solver, implemented in the Simulink simulation environment using MATLAB's S-function.

Summarizing, it can be stated that the most significant contradictions remaining in controlling combined propulsion systems are:

– the working space of the designed controllers is limited by the movement of the vessel in the horizontal plane;

– motion control is carried out at low speed, i.e., the ship moves at speeds less than 2 m/s to reduce the impact of nonlinear effects;

– measuring and estimating the vessel's position and speed is crucial for accurate traffic management. This task is made increasingly difficult by the deterministic motion caused by the waves. Thus, when designing a controller, it is assumed that all states are evaluated using an existing algorithm or measured directly;

– existing results include only the development of MCS controllers because the integration methods were not investigated. In addition, the algorithmic aspects of solving the problem of nonlinear control were not considered;

– in order to reduce the complexity of mathematical modeling and setting, mainly one specific vessel with a given configuration of THR PDA was considered in the studies.

A solution to these contradictions could be the development of a predictive control system using a high-level controller. This is the approach used in many works; however, due to the uncertainty of the boundary conditions and the need to divide the system, the achieved results are not perfect. This is primarily due to non-identical methods for measuring the parameters of distributed subsystems and the corresponding conditions for achieving a certain level of adequacy. Secondly, the variety of THRs and their location requires the parameterization of both the THRs themselves regarding the determination of input control signals and the coordination of input-output signals between distributed subsystems. All this gives reason to assert that for ship combined propulsion systems it is expedient to conduct the researching aimed at designing a predictive control system.

3. The aim and objectives of the researching

The purpose of our researching is to design an energy-efficient system for predictive control over a multi-level controller in a closed system of ship motion control. The practical result should be the construction of a reference controller combining a multi-level motion controller and the THR control algorithm depending on the location matrix and, finally, increasing the functionality of a closed system to the level of a combined controller.

To solve these problems, the following tasks must be solved:

– to define the law of optimal control over a multi-level nonlinear MPC-controller taking into account the dynamic properties of an sea-based vehicle (SBV) model;

– to test various configurations of thrusters to find optimum settings and control errors from the point of view of energy saving in the zone at the point of positioning and movement at low speeds.

4. The materials of researching and methods

4. 1. The object and hypothesis of the researching

The object of our researching is the process of maneuvering a sea-based vehicle (SBV) with 6 degrees of freedom, which moves in accordance with the laws described in Table 1. Fig. 1 shows the hierarchical structure of the ship's automated traffic control system.

The main hypothesis of the researching assumes the improvement of accuracy of maintaining SBV, which works under the mode of dynamic positioning, through the use of predictive control methods and tools using a high-level controller.

In order to positively solve the tasks, the controller must be expanded by including in the circuit the module for the distribution of thrusts between the THR motors, which solves the combined problem of motion and THR control. The controller will be considered as a reference for the closed control system of the ship. Based on the preliminary results, it is planned to improve the energy efficiency of the closed-loop system by incorporating more information into the high-level MPC controller.

Based on analysis of the theory of predictive control and theoretical studies of ship dynamics and dynamic positioning, for the researching of the dynamic positioning mode, a general model describing the dynamics of the ship is represented by the expressions:

$$\dot{\eta} = J(\eta)\nu, \tag{1}$$

$$M\dot{\nu} + C(\nu)\nu + D(\nu)\nu + g(\eta) = \tau, \tag{2}$$

where (1) describes the kinematics of SBV, and (2) describes the kinetics. The matrix $J(\eta)\in R^{6\times 6}$ is the transformation matrix, while the matrices $M\in R^{6\times 6}$, $C(\nu)\in R^{6\times 6}$ and $D(\nu)\in R^{6\times 6}$ describe the inertia of the attached masses, the Coriolis force, and the vehicle damping, respectively. The vector $g(\eta)\in R^6$ describes the restoring forces acting on the vehicle due to buoyancy and gravity. In the right-hand side of (2), $\tau\in R^6$ is a vector of forces and moments created by controlling elements of propulsion devices and factors of the external environment (wind, waves, currents) and acting on SBV during a certain operating mode:

$$\tau = \tau_c + \tau_{env}, \tag{3}$$

where τ_c are the controlling forces and moments, and τ_{env} are the forces and moments arising as a result of environmental disturbances.

Table 1

A system of parameters or variables for different coordinate systems depending on the degrees of freedom (DOF) of the ship or underwater vehicle

No. of entry	DOF	Defining a parameter or variable	Description
1	6	$\eta = [xyz\phi\Theta\psi]^T \in R^6$	Orientation of SBV according to 6 degrees of freedom, given position, and Euler angles in the inertial system
2		$\nu = [xyzpqr]^T \in R^6$	Linear and angular velocities in a fixed body coordinate system
3		$\tau = [XYZKMN]^T \in R^6$	Decomposition of forces and moments for a fixed body coordinate system
4	3	$\eta = [xy\psi]^T \in R^3$	Horizontal orientation with 3 degrees of freedom given by the Cartesian position (x, y) and the heading angle ψ
5		$\nu = [uvr]^T \in R^3$	The vessel's velocities in a fixed coordinate system during rectilinear motion (u), pitching (υ) and yaw (r), respectively
6		$\tau = [XYN]^T \in R^3$	Forces and moments in a coordinate system assigned to a body during accelerations (X), oscillations (Y) and turns (N), respectively.

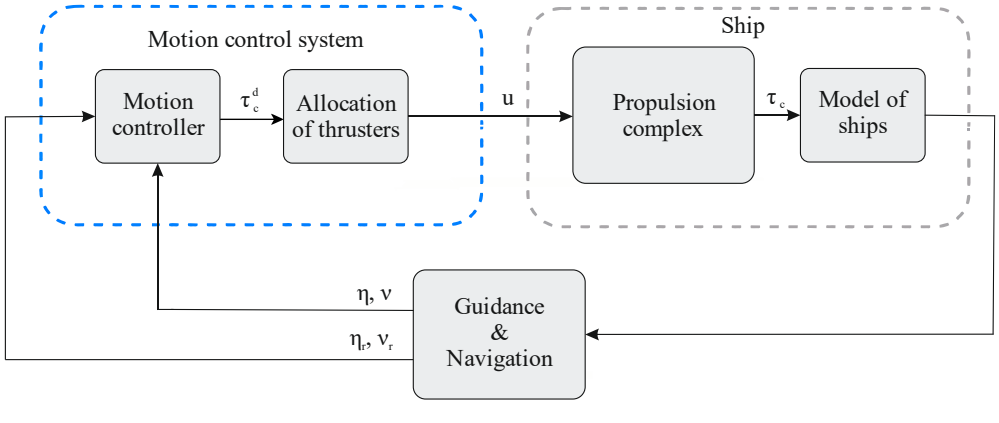

Fig. 1. Hierarchical structure of the ship's automated traffic control system

However, these assumptions relate to the control over the position and course of the control object on the surface of the water, that is, for the improvement of this component of the control system and to reduce the power of mathematical models, only horizontal movement is considered. Thus, the model given in (1), (2) reduces to 3-DOF. Motion at yaw z, pitch θ, and roll φ is not tracked or compensated for at this stage.

4. 2. Generalization of kinematic relations taking into account degree restrictions

Two different coordinate systems were used in the simulation. An inertial (non-moving) coordinate system used to describe the position and orientation of a vessel in global coordinates and Euler angles as $[x\ y\ z]^T$and $[\phi\ \theta\ \psi]^T$, respectively. A moving coordinate system describing forces, torques, linear velocities, and angular velocities $[X\ Y\ Z]^T$, $[K\ M\ N]^T$, $[u\ v\ w]^T$, $[x\ y\ z]^T$, as well as $[p\ q\ r]^T$ respectively. A moving coordinate system, the variables are denoted by the index {b}, is usually related to SBV through the reference point that is at the center of gravity, and the x_b axis is directed forward, towards the bow, the y_b axis is the starboard side, and the z_b is directed downwards [10]. Fixed coordinate system – Cartesian local tangent coordinate system NED (North-East-Down), variables are marked with the index {n}. The origin of the coordinates is fixed at a point on the Earth's surface, the x_n axis is directed to the north, the y_n axis is to the east, and the z_n axis is to the center of the Earth. In this chapter, the NED-system is assumed to be inertial, which is appropriate in view of the fact that the considered velocities are involved in the motion control laws at relatively low speeds. A general visual description of the applied coordinate systems, which characterizes the connection between the NED and the moving coordinate system with decomposed velocities, is shown in Fig. 2.

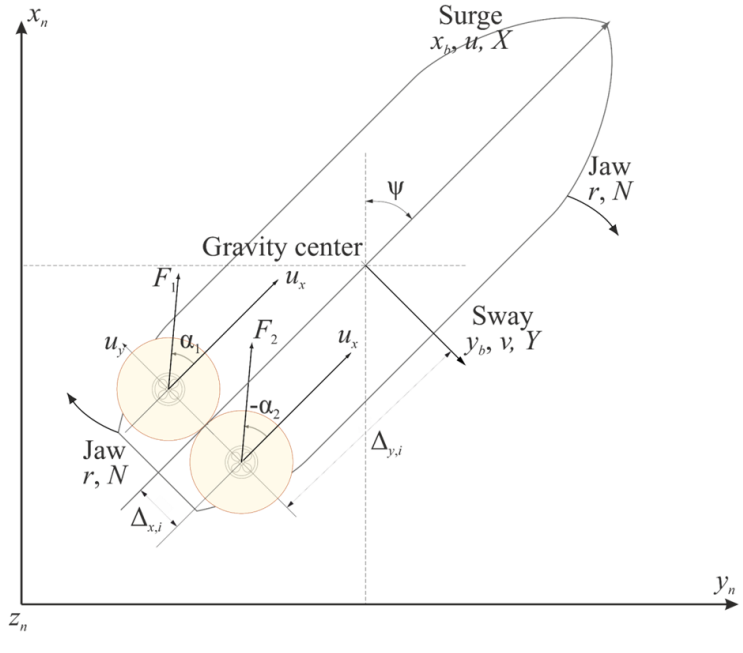

Fig. 2. Velocities plotted in the stationary coordinate system of a sea-based vehicle: ψ – heading angle

The position and heading η of the vessel is measured in {n}, while the velocities ν and forces τ will be plotted in {b} (Fig. 2). This is the basis for purely geometric transformations of the matrices in (2), which as a result reduces to:

$$\dot{\eta} = R(\psi)v, \tag{4}$$

for 3-DOF, where $R(\psi)\in R^{3\times3}$ is the rotating matrix given by:

$$R(\psi)\begin{bmatrix}\cos(\psi) & -\sin(\psi) & 0\\ \sin(\psi) & \cos(\psi) & 0\\ 0 & 0 & 1\end{bmatrix}. \tag{5}$$

Kinetics describes the movement of a body under the action of forces and moments. The model of SBV kinetic movement can be derived using the mechanics of a solid body and the theory of hydrodynamics [2, 14]. When considering the motion of SBV in 3-DOF, (2) together with (3) reduces to:

$$M\dot{\nu} + C(\nu)\nu + D(\nu)\nu = \tau_c + \tau_{env}, \tag{6}$$

where M, $C(\nu)$ and $D(\nu)\in R^{3\times3}$.

For the purpose of controller design, it is often convenient to work with linear models [15, 16]. For restrictions on low velocities and taking into account the quadratic dependence of non-constant terms in $C(\nu)$ and $D(\nu)$, equation (6) can be simplified to a linear dynamic equation:

$$M\dot{\nu} + D(\nu)\nu = \tau_c + \tau_{env}. \tag{7}$$

If we assume that SBV is symmetric in the x_bz_b plane with the origin {b} coinciding with the center of gravity, then the corresponding matrices, as a rule, have the following structure:

$$M = \begin{bmatrix}\times & 0 & 0\\ 0 & \times & \times\\ 0 & \times & \times\end{bmatrix},\quad D = \begin{bmatrix}\times & 0 & 0\\ 0 & \times & \times\\ 0 & \times & \times\end{bmatrix}, \tag{8}$$

in such a way that translational movement is separated from pitching and yaw. The matrix elements in M are derived from the mechanical properties of the specific SBV, such as mass and inertia, as well as from hydrodynamics, which describes the behavior of the attached water masses, while the elements in D are purely derived from hydrodynamics.

Summarizing the above, it can be stated that the simplified model of SBV dynamics for 3 degrees of freedom is found by combining (4) and (7), as:

$$\dot{\eta} = R(\psi), \tag{9}$$

and

$$M\dot{\nu} + D\nu = \tau_c + \tau_{env}, \tag{10}$$

with states $[\eta^T\ \nu^T]^T$ and input τ_c. The model can be written as a spatial model of states by permuting (10) with multiplication of both parts of the matrix by the inverse matrix M.

4. 3. Mathematical modeling of propulsion devices taking into account the number of degrees of freedom

Model Predictive Control (MPC) is based on a strategy whose main features include the ability to control systems with multiple inputs and multiple outputs using an internal model. Performance techniques are used to predict future states and

the ability to handle constraints on states and inputs such as supply voltage or resistance torque level.

SBV can be equipped with THR of various types, the main purpose of which is to create a controlled thrust force to obtain the desired movement. At low-speed traffic control, azimuthal THRs are most often used. In this case, the modeling assumes a quadratic relationship between the thrust and the control variable, which makes it common for most THRs of this type.

The control forces and moments τ_c created by THR depend on its location and orientation relative to the diametrical plane and on the absolute value of the created force (thrust). Thus, in the general case, for the M matrix THR τ_c can be written as:

$$\tau_c = h(\alpha, n), \tag{11}$$

where $\alpha \in R^M$ is a vector of thruster location angles, $n \in R^K$ is a vector of propeller speeds. For low speeds, h usually takes the following form [10]:

$$\tau_c = T(\alpha) f(n), \tag{12}$$

where $f(n) \in R^M$ is the thrust magnitude vector for each THR motors, and:

$$T(\alpha) = [t_1, ..., t_N] \in R^{n \times M}, \tag{13}$$

describes the geometry of the motor configuration. For n=3-DOF, columns $T(\alpha)$ are set as:

$$t_i(\alpha_i) = \begin{bmatrix} \cos(\alpha_i) \\ \sin(\alpha_i) \\ \Delta_{x,i}\sin(\alpha_i) - \Delta_{y,i}\cos(\alpha_i) \end{bmatrix}, i = 1, ..., M, \tag{14}$$

where $\Delta_{x,i}$ and $\Delta_{y,i}$ are the arm of moment application, specified in the fixed body coordinate system, and α_i determines the angle of location of THR, such that it is positive clockwise from the x_b axis, Fig. 3.

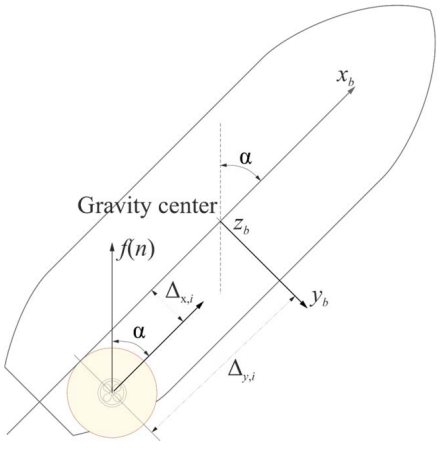

Fig. 3. Determining the application of moments and orientation of a vessel equipped with an aft thruster

For low-speed motion control, it is assumed that the thrust f generated by the THR motor is proportional to the square of the propeller rotation speed. More precisely, under the condition of thrust from bollard (stationary vessel), the steady axial thrust $f(i)$ of the i-th THR motor with symmetrically located propellers is defined as:

$$f_i = k_i n_i |n_i|, i = 1, ..., M, \tag{15}$$

where k_i is a constant and n_i is the angular speed of the propeller. Subsequently, the thrust vector $f(n)$ in (12) can be written in the following form:

$$f_n = \begin{bmatrix} f_1(n_1) \\ . \\ . \\ . \\ f_M(n_M) \end{bmatrix} = K \begin{bmatrix} n_1|n_1| \\ . \\ . \\ . \\ n_M|n_M| \end{bmatrix}, \tag{16}$$

where $K \in R^{M \times M}$ is a diagonal matrix with $[k_1, k, ..., k_N]$ along the diagonal. However, it should be noted that, in general, the generated thrust of THR depends on the speed of the liquid around the propeller, which, in turn, is related to the speed of the vessel [17–19].

It was established that the thrust created by the propeller is proportional to the square of the speed of rotation, according to some assumptions. This is also true for the applied torque [20]. It is known from mechanics that the THR power P is proportional to the torque T at rotation frequency ω.

Thus, a general approximation for the power required to rotate the propeller is:

$$P \infty n^3, \tag{17}$$

where n is the speed of rotation of THR propeller, rev/min. In addition, the above ratio usually holds for open water conditions, that is, the propeller is under the influence of an unobstructed and uniform flow of water.

For azimuthal THRs, this may not be the case, when the thrust is achieved through the reverse rotation of the propeller. Additionally, propellers are sometimes designed to be more efficient in one direction than another. Thus, the efficiency of a THR motor may vary depending on whether it is reversible or not. Such THR motors are asymmetrical.

Decomposition of control over asymmetric THRs is a method often used in aerospace and marine engineering to control the redundancy of drives in the design of dynamic systems operating under operational modes with overload [21–23]. The control system is then partitioned by a law that determines the total control effort to be generated and a control distribution algorithm that distributes the effort among the actuators. The control distribution is identified with respect to the THR motor, with the goal of distributing the desired generalized force τ_c^d between the THR motors. Thus, the main principle of THR location is τ_c^d implementation at any time. However, due to the redundancy in actuation, there is freedom in the choice of the method of distribution of forces, that is, the choice of the control input u=(n, α). The more THRs the ship is equipped with, the more combinations of input data can be used to obtain τ_c^d. The problem of choosing the input parameter u is naturally solved by formulating it as an optimization problem, in which the cost function usually involves the minimization of fuel or energy consumption, and the constraints take into account the limitations of a particular THR motor and its wear resistance [2, 24–26].

Perhaps the simplest form of distribution of THR thrusts can be found in the combined solution of (12) and (16). Changing the variable $\upsilon_i = n_i|n_i|$ occurs by introducing the unique inverse $n_i = \text{sign}(\upsilon_i)\sqrt{|\upsilon_i|}$, which leads to the ratio:

$$\tau_c^d = T(\alpha) K v, \tag{18}$$

between the desired task of thrust from the motion controller τ_c^d and the control tasks of THR drive n and α. Taking into account the fact that α is a constant value, that is, THR motors have a fixed orientation relative to the diametrical plane, $T(\alpha)K$ is also constant. If the physical limitations of THR position are not considered, then the optimization problem can be stated as a weighted least squares problem:

$$\min_v v W v^T,$$
$$s.t. \tau_c^d - Hv = 0. \quad (19)$$

The solution is found by differentiating and setting the operational zero, as follows:

$$v = W^{-1}H^T\left(H^T W^{-1} H\right)^{-1}\tau_c^d. \quad (20)$$

If $W=I$, then the solution to (20) reduces to the pseudo-inverse Moore-Penrose matrix.

However, when considering azimuthal THRs, α is not constant. In addition, it is not guaranteed that a given THR arrangement is capable of providing the desired thrust force τ_c^d, if this requires a force that exceeds the capabilities of THR motors, for example due to saturation. The generalized statement of the problem will be as follows:

$$\min_{u,s} p(\eta, v, u, s, t),$$
$$s.t. \tau_c^d - h(\eta, v, u, t) = s, \quad (21)$$
$$g(\eta, v, u, t) = 0,$$

where p is some function of evaluating states (η, ν), inputs $u=(n, \alpha)$, delay variables s and time t. The constraint p in (21) represents the main priority of the motor thrust distribution, but with the addition of s in case this is not possible.

For prioritization, the delay variable usually has a much higher weight in p than the other variables. For low speed, the function h is usually represented by the right-hand part of (12). The constraints in (21) represent technical constraints of THR, such as torque or power constraints.

In general, the problem of distribution of thrusts and moments of THR motors (21) is unsolved. This means that the optimization solution may stop at some local minimum. For asymmetric THRs, which are designed for maximum efficiency in one direction, but are not as efficient when rotating in the opposite direction, this means that the THR may end up not providing the required thrust. This problem can be solved in various ways, in particular, a common approach is the presence of an exogenous algorithm that evaluates whether the rotation of THR motor is effective for a certain operating mode [10].

5. Results of investigating the method of predictive control over a ship model with azimuth propulsion devices

5. 1. Defining the law of optimal control over a multi-level nonlinear MPC controller taking into account the dynamic properties of SBV model

The difference between linear and nonlinear *MPC* is that the latter can work with nonlinear dynamics and constraints. In either case, the control input is computed by solving a finite value optimal control problem at each sampling interval. In continuous time, the law of optimal control can be formulated as follows:

$$\min_{u(\cdot)} \int_{t_0}^{t_0+T} f\left(t, x(t), u(t), x_r(t), u_r(t)\right)\mathrm{d}t +$$
$$+ f_N\left(x(t_0+T), x_r(t_0+T)\right),$$
$$s.t. \quad \begin{array}{l} x(t_0) = x_0 \\ \dot{x}(t) = f\left(x(t), u(t)\right) \\ g\left(t, x(t), u(t)\right) \le 0, \forall t \in [t_0, t_0+T] \end{array} \quad \forall t \in [t_0, t_0+T], \quad (22)$$
$$f(\bullet) = \left\|x(t) - x_r(t)\right\|_{Q_x}^2 + \left\|u(t) - u_r(t)\right\|_{Q_x}^2,$$
$$f_N(\bullet) = \left\|x(t) - x_r(t)\right\|_{R_x}^2,$$

where $x(t) \in R^{nx}$ are the system states, and $u(t) \in R^{nu}$ are the control inputs. Input data for the controlled optimal control system are the current state estimate x_0 and the reference trajectories $x_r(t)$ and $u_r(t)$, $\forall t \in [t_0, t_0+T]$. The task of the controller is determined by the energy loss function (22), which here consists of two terms: current losses $f(\cdot)$ and final $f_N(\cdot)$. The function of the final losses is to estimate their achievement of the final state $x(t_0+T)$, while the current losses represent the task and the losses to achieve this task. A common way to construct terms and loss bounds is to use a least-squares objective function, weighting the difference between the states, the inputs, and the corresponding constraints:

$$f(\bullet) = \left\|x(t) - x_r(t)\right\|_{Q_x}^2 + \left\|u(t) - u_r(t)\right\|,$$
$$f_N(\bullet) = \left\|x(t) - x_r(t)\right\|_{R_x}^2. \quad (23)$$

Dynamic models used for predicting are given by formulas for continuous quantities (22), which contain given system constraints. The design variables include the prediction limit T, which determines how optimal the controller is from the point of view of prediction, and the weight matrices $Q_x \ge 0$, $Q_u > 0$ and $R_x \ge 0$, which determine the entries of the tasks in the loss function.

However, to solve (22), it must be discretized. There are a number of different discretization methods for continuous systems, such as Euler sampling and Runge-Kutta methods. The discrete version of (22) taking into account (23) with the sampling frequency $1/T_s$ is:

$$\min_{U_t} \sum_{k=0}^{N-1} \left\|x_{i+K} - x_{i+K}^{ref}\right\|_{Q_x}^2 +$$
$$+ \left\|u_{i+K} - u_{i+K}^{ref}\right\|_{Q_u}^2 + \left\|x_{i+N} - x_{i+N}^{ref}\right\|_{R_x}^2,$$
$$x_i = 0,$$
$$s.t. x_{i+K+1} = f_d\left(x_{i+K}, u_{i+K}\right), K = 0, ..., N-1,$$
$$g_{d,i}\left(x_{i+K}, u_{i+K}\right) \le 0, k = 0, ..., N-1, \quad (24)$$

where $N=T/T_s$. The solution that is the minimum of (24) at time i is the trajectory of the control inputs $U_i^* \in R^{N \times nu}$. This trajectory is computed in an open loop and only the first

element in U_i^*. is used to achieve feedback. Then the system expands, and the problem is solved again in the next sampling interval i+1. Since the optimization problem is solved at each sampling interval, predictive control systems tend to be computationally complex. The complexity of the problem increases with the number of states and inputs and the range and prediction vector N. Thus, there is a trade-off between a large range and prediction vector and a fast controller.

In the case of a linear model, the system of equations (24) is subject to the following restrictions:

$$x_{k+1} = Ax_k + Bu_k,$$

$$F_x x_k \le b_x,$$

$$F_u u_k \le b_u. \qquad (25)$$

(24) can be reformulated as a quadratic programming (QP) problem. Then the optimization problem is convex from the point of view of the global optimal solution. Solving the nonlinear problem (24) is complicated by the fact that the optimization problem in the general case becomes nonconvex. One common approach to solving nonconvex problems is to linearize the system around some point, such as a reference point, and then formulate a standard QP. This allows the solver to find a global solution to the approximated problem. Other methods, such as Sequential Quadratic Programming (SQP), use sequential iteration to solve numerous QP problems, bringing the nonlinear program closer to convergence. Instead, the ACADO toolkit exports a Real Time Iterations (RTI) scheme for optimization aimed at providing an approximate but fast solution. The RTI scheme essentially works by linearizing the problem around estimating the current state and solving one QP at each iteration, thus making it only marginally slower than linear MPC [13].

Therefore, the law of optimal control over a multi-level nonlinear MPC-controller, taking into account the dynamic properties of SBV model, is defined in continuous time with dependence on t for states and control elements. The problem is discretized using either the ACADO toolkit, where it is possible to export both individual explicit and implicit integration methods, or for controllers, nonlinear MPC is used.

5. 2. Testing different configurations of thrusters to find optimum settings and control errors

MPC is a high-level motion controller whose dynamic model (9) and (10) is used for prediction, but with substitution instead of τ_c since the latter does not directly affect the ship (Fig. 4).

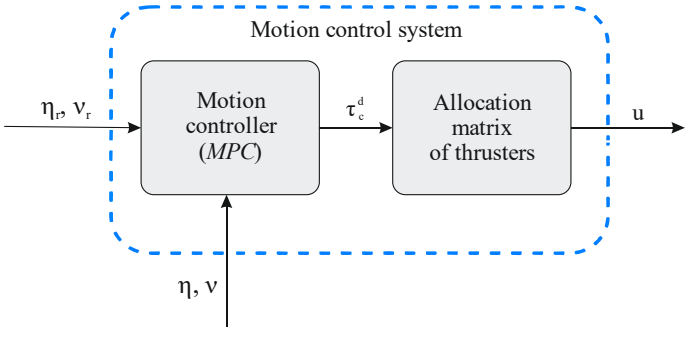

Fig. 4. Separate motion control system

SBVs maneuvering at low speeds or operating under THR mode are, as a rule, equipped with an excess number of THRs from the point of view of ensuring continuity, which means the existence of more than one or the same number of control input signals n_u for the corresponding number of degrees of freedom n [10, 17]. This makes it possible to increase the accuracy of controlling the ship in the horizontal plane and, in the case of redundancy, to maintain controllability in case of failure of one or more THRs. The method implementation procedure consists of the description of the management hierarchy and the implementation of this hierarchy using a non-linear model of predictive control and iterative elimination of deficiencies depending on the obtained results.

The conventional *MCS* for SBV is divided into several levels. First, the high-level motion controller takes the measured or estimated state of the vessel (η, ν) and the reference signal (η_r, ν_r) as inputs. The reference signal can be a reference value, a path, or a trajectory. Then the task is to calculate the desired generalized force applied to the vessel τ_c^d, corresponding to the reference task. Several different algorithms have to be developed for this purpose, ranging from decoupled *PID*s to linear-quadratic and nonlinear controllers. Secondly, the algorithm for the distribution of THR thrusts is designed to create the desired force τ_c^d by controlling the speed and orientation of the THR u=(n, α) (Fig. 1).

MPC is a high-level motion controller whose dynamic model (9) and (10) is used for prediction, but with substitution of τ_c^d, instead of τ_c since the latter does not directly affect the ship (Fig. 4).

To apply physical constraints to the ship and the DP system, the input signal τ_c^d, must be limited both in amplitude and speed, which is implemented by supplementing the model with:

$$\dot{\tau}_c^d = T_c\left(-\tau_c^d + \tau_a\right),$$

$$\dot{\tau}_a = u_\tau, \qquad (26)$$

where $T_c \in R^{n\times n}$ is the diagonal matrix of time constants, and u_τ is now the control variable. Thus, the speed limitation τ_c^d can be formulated as a limitation of the value of u_τ.

By combining the dynamic model (9) and (10) with (26) together with the constraints, the nonlinear continuous time optimal control law is formulated as follows:

$$\min_{u_\tau} \int_0^{T_s N} \left(\left\|\eta-\eta_r\right\|_{Q_\eta}^2 + \left\|v-v_r\right\|_{Q_v}^2 + \left\|\tau_c^d\right\|_{Q_\tau}^2 + \left\|u_r\right\|_{Q_{d\tau}}^2\right)dt,$$

$$s.t. \dot{\eta} = R(\psi)v,$$

$$M\dot{v} + Dv = \tau_c^d,$$

$$\dot{\tau}_c^d = T_c\left(-\tau_c^d + \tau_a\right),$$

$$\dot{\tau}_a = u_\tau,$$

$$\underline{\tau}_c^d \le \tau_c^d \le \overline{\tau}_c^d,$$

$$\underline{u}_\tau \le u_\tau \le \overline{u}_\tau, \qquad (27)$$

where obtaining the final value involves the same conditions as the intermediate ones. The intermediate functions in (27) allow time to be changed by η and ν, while the magnitude of the generalized force and its speed are adjusted accordingly. Weight matrices Q_x can be changed depending on the control strategy. For ex-

ample, if it is necessary to move along a trajectory, the course ψ and the longitudinal movement u can be adjusted more precisely by simultaneously adjusting the weights τ_c^d along the corresponding (x, y) axes. The constraints in (27) determine the dynamic model and limit the magnitude and speed of the generalized force τ_c^d.

The efficiency of control is checked in the simulation using the appropriate model of the multifunctional propulsion system for the variant of operation of two THRs of the Azipod® type, maximally spaced relative to the diametrical plane of the vessel (Fig. 5). The results are summarized in Fig. 6, where the movement of the model in two directions is visualized.

Parameters of the physical model are shown in Fig. 5, given in Table 2.

The differences between the simulations lie in the reference position and initial orientation of the initialized THR motors (Table 3).

The results of the first test run for the separate *MCS* control mode are shown in Fig. 7, 8.

The results of the second test run for the separate *MCS* control mode are shown in Fig. 9, 10.

The setting parameters remain constant during the simulation, during which deviant actions are performed to provoke the deviation of THR parameters from the specified ones. The environmental perturbation τ_{env} was not applied in all simulations in order to emphasize the vessel behavior for the separate (autonomous) nature of MCS.

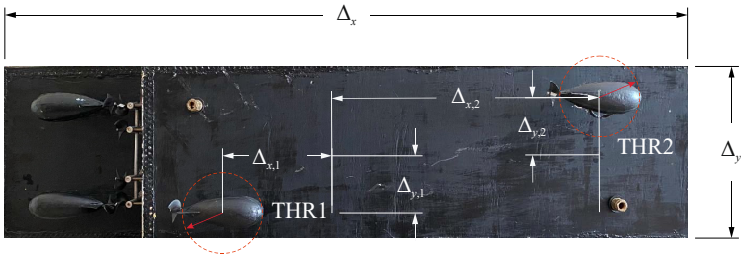

Fig. 5. Model of a multifunctional propulsion system

Table 2

Parameters of the physical model of the multifunctional propulsion system and initialized propulsion devices

No. of entry	Parameter	Value	
1	Length, Δ_x	140 cm	
2	Width, Δ_y	40 cm	
3	Draft	20 cm	
4	Displacement	243 kg	
		PD1	PD2
5	$\lvert\Delta_x\rvert$	38 cm	64 cm
6	$\lvert\Delta_y\rvert$	16 cm	16 cm
7	Azimuthal rotation time	22 s	22 s
8	Maximum propeller speed	±145 rpm	±145 rpm
9	Maximum acceleration of propeller speed	±0.06 rev/s^2	±0.06 rev/s^2

Table 3

Summarized data on the parameterization procedure of initialized thrusters

No. of entry	Starting position of the model	Start location angle of THR	Reference position pitch η_r	Time constant T_s, c	Forecast horizon N, c
1	$[-50, 0, 0]^T$	$[0, 0]^T$	$[80, 0, 0]^T$	1	80
2	$[-10, 40, 0]^T$	$[\pi/2, \pi/2]^T$	$[0, -50, 0]^T$	1	80

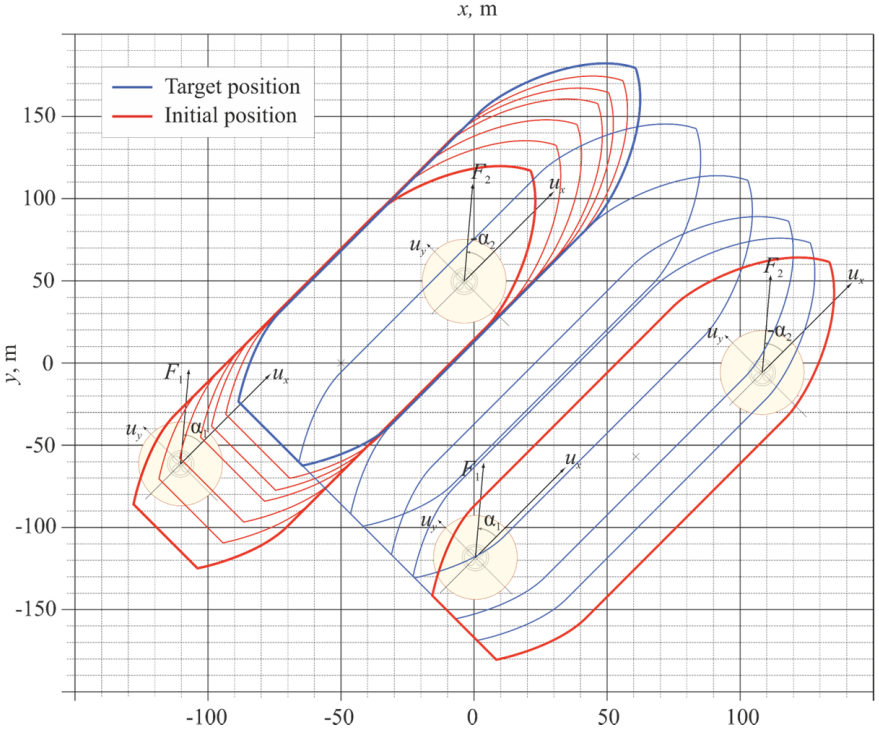

Fig. 6. Image of the movement of the model in the horizontal plane

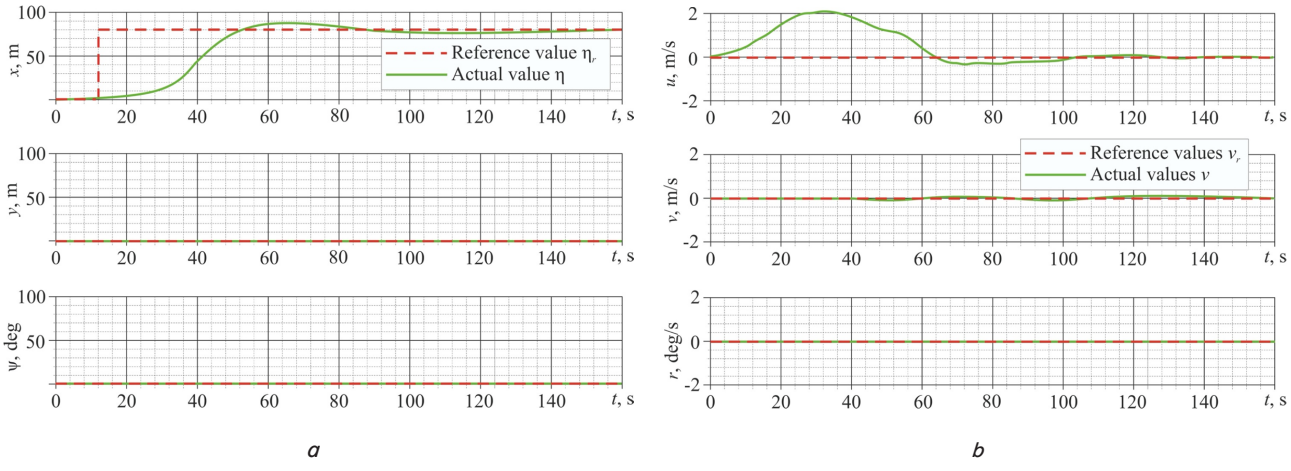

a *b*

Fig. 7. Results of the first test for the separate mode of the motion control system: *a* — reference (ηr) and actual (η) values of ship's position in accordance with the number of degrees of freedom; *b* — the actual (v) and reference (vr) value of the speed of the model

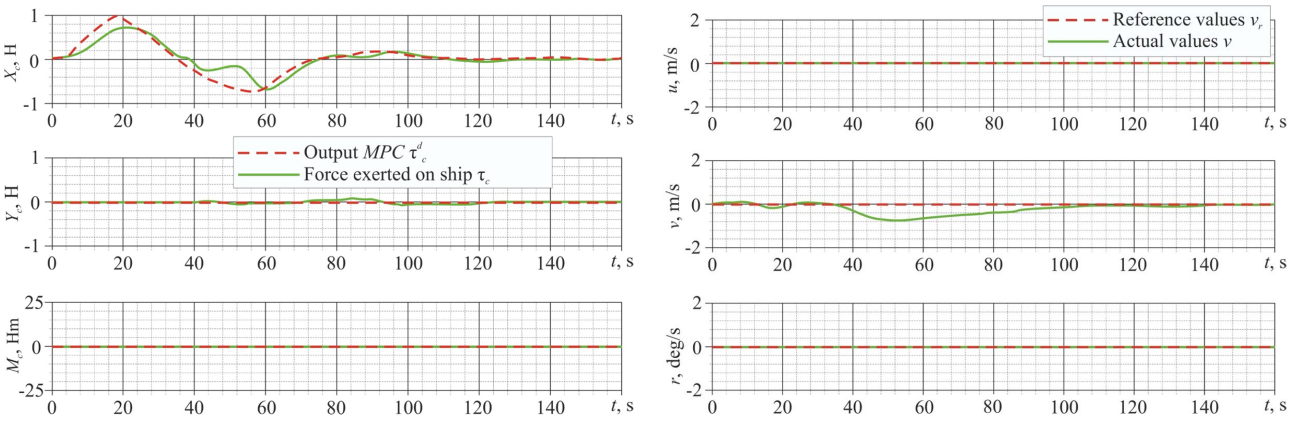

a *b*

Fig. 8. Results of the first test for the separate mode of the motion control system: *a* —dependence of the force acting on the ship (τc) and the task at the output of the high-level control controller $\left(\tau_c^d\right)$; *b* — dependences of the rotation frequency of the propellers (n) and the location angle (α) of thrusters within [±180°]

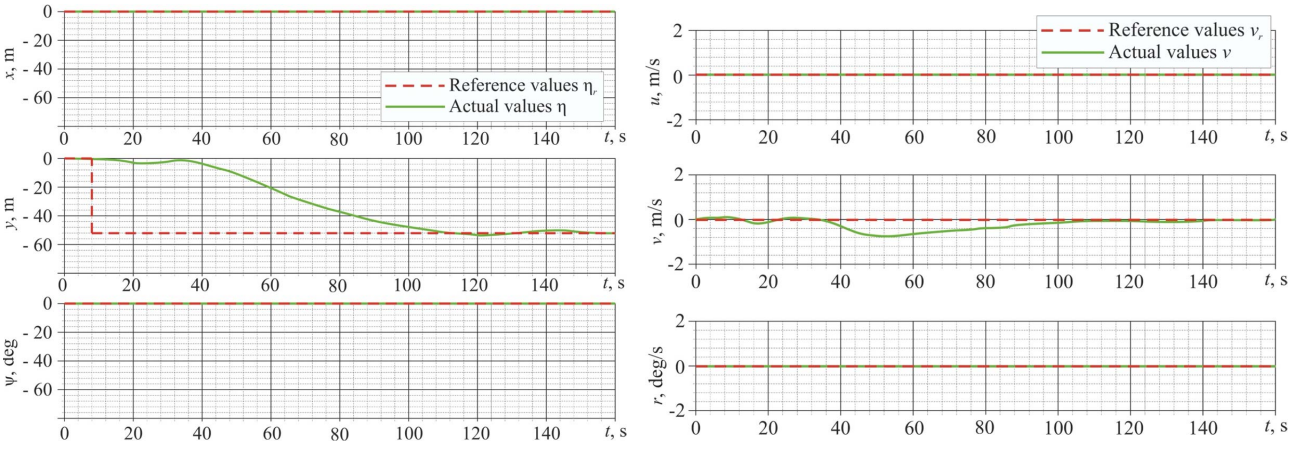

a *b*

Fig. 9. Results of the second test for the separate mode of the motion control system:
a — the reference (η_r) and actual (η) values of ship's position depending on the number of degrees of freedom;
b — the actual (*v*) and reference (v_r) value of the speed of the model

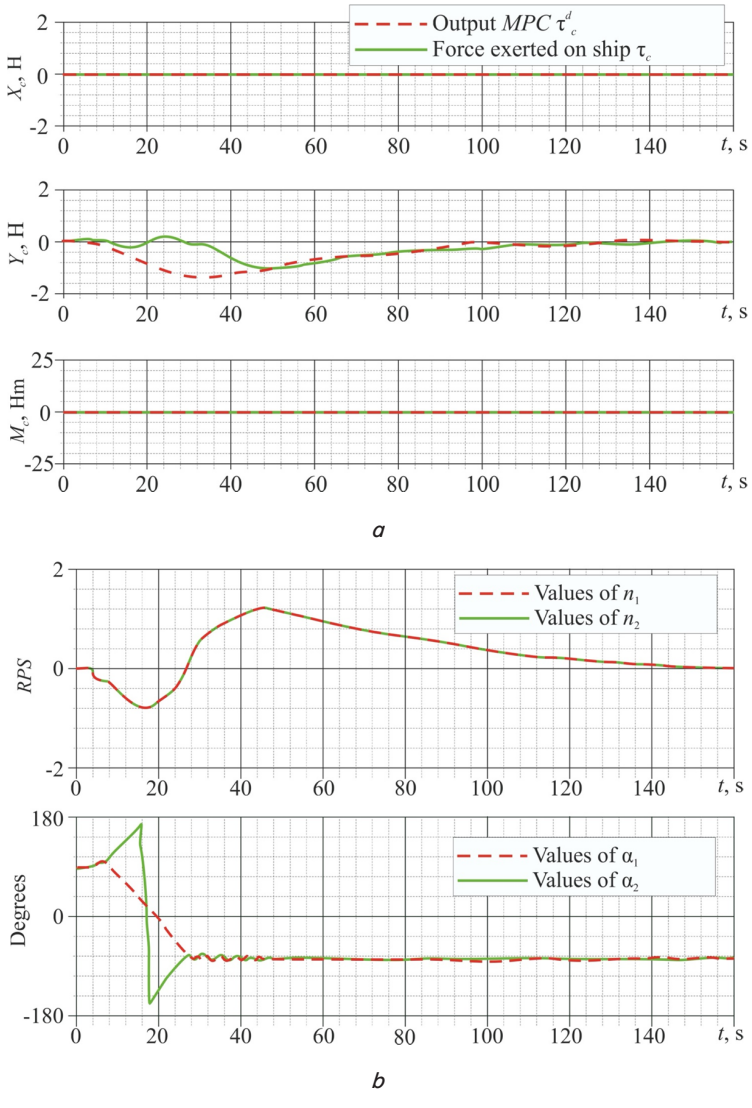

Fig. 10. Results of the second test for the separate mode of the motion control system: *a* — dependence of the force acting on the ship (τc) and the task at the output of the high-level control controller $\left(\tau_c^d\right)$; *b* — dependences of the rotation frequency of the propellers (n) and the location angle (α) of thrusters within [±180°]

6. Discussion of results of investigating the predictive control over a ship model with azimuth propulsion devices

The law of optimal control over the multi-level nonlinear MPC-controller, taking into account the dynamic properties of SBV model, has been implemented using a low-speed algorithm with the location of THR for option (21). The results for this case are, first of all, explained by the possibility of asymmetric arrangement of THR (Fig. 5). Thus, in an attempt to instantly reach the desired thrust, the simultaneous rotation of the THR motors with a rotation frequency that is considered positive counterclockwise is used to minimize energy consumption.

From Fig. 5, it becomes clear that unlike the solutions proposed in [2, 10, 15, 17], THRs provide thrust with all three degrees of freedom since THR motors can rotate in any direction. However, depending on the orientation of THR, at some moments the thrust in a certain direction may be zero. These restrictions in (27) are quite difficult and ambiguous to define. For the case when the flows from the THR motors are stationary (constant angle α), one uses (12) taking into account the specification of a specific THR to calculate the corresponding limits of the amplitude and the rate of increase of the task τ_c^d. This becomes possible due to the fact that the specified limits are considered more as tuning parameters than actual physical limitations.

Testing of different configurations of thrusters to find optimum settings, control errors and *MCS* modes was performed in a wide range of maneuvering for cases of reference speed v_r=0 and reference position step η_r at t=8. In the first case, the model control system receives a command to move to the position in front of it and a command to stop.

The THR motors are initially directed in the direction of movement. The results of the experiment are shown in Fig. 7, 8. Fig. 7, *a* shows a significant uncontrolled exit of the model beyond the target position. However, during simulation, the positive result is the realistic movement of the ship in the opposite direction, which is the reason for the negative speed of the wave u in Fig. 7, *b*. The understanding of this behavior of the vessel can be seen by considering Fig. 8, *a, b*. At t=38 s, both THR motors rotate in the same direction, for example, clockwise (Fig. 8, *b*). At the same time, the high-level MPC begins to send a command to "reverse" (Fig. 8, *a*), and the THR motors change the direction of rotation. However, after a few seconds, the rotation of the THR motors should be up to the task τ_c^d. This means that the ship will not be able to create a propulsive force to overcome the drag moment in accordance with the rotation of THR. The main drawback of the researching is a significant discrepancy between τ_c and τ_c^d, as shown in Fig. 8, *a* for $t\in$[50, 70] since this lies outside the *MPC* setting. In fact, a similar discrepancy in forces can be observed during $t\in$[100, 120] seconds, when the MPC forms a command to reduce the ship's speed at the moment of changing the direction of rotation of THR motors, which leads to a slight discrepancy in the ship's position from the given one (Fig. 8, *a*) . The length of the duration is related to the inaccuracy of the regulation of the rotation speed of THR motors. The solution to this problem can be achieved through the use of feedback on the coordinates of THR electric motors.

In the second case, the model should move in the opposite direction y_b. Detailed results are shown in Fig. 9, 10. The motors are directed from the beginning and are located in the direction y_b, which coincides with the direction of movement (Fig. 10, *b*). A limitation of this researching is that at the time of the target position assignment, the MPC immediately requires a large negative oscillating force because the orientation and physical constraints of THR motor system are not specified (Fig. 10, *a*). This leads to a significant discrepancy between the desired and the actual force acting on the vessel. In an attempt to execute τ_c^d, immediately, the THR's position control system begins to rotate THR's motors in the opposite direction, simultaneously rotating the motors to minimize energy consumption. This disadvantage is due to the fact that when the motors are pointed aft and bow respectively, at t=20, there is no point in moving the motors in the opposite direction

since it is impossible to get the corresponding thrust. Thus, the control system over the position of THRs begins to slow down the movement of the THRs, continuing to rotate them towards the left side. However, due to the insufficient deceleration of THR movement, the ship continues to move in the opposite direction y_b. The position of the vessel is shown in Fig. 9, *a*, and the speed – in Fig. 9, *b*. This, from the point of view of energy consumption, is a negative result. Although, unlike the first scenario, in this case, the distance relative to the reference position was not exceeded since the *MPC* does not issue a signal to reduce the speed of the vessel due to its lower value and greater movement resistance. It is possible to eliminate this shortcoming through the use of more accurate algorithms for pulse-width modulation of voltage on THR electric motors, which could improve energy efficiency by reducing the coefficients of higher harmonics in voltage [27–30].

7. Conclusions

1. The law of optimal control over a multi-level nonlinear MPC controller with a separated mode of MCS operation reveals advantages due to the modular method of software organization. However, taking into account the dynamic properties of SBV model, the performance of MCS may decrease due to the inability of the high-level controller to take into account the magnitudes of the generated forces. The THR position control system algorithm must take into account the direction and frequency of rotation of the THR motors to achieve the force requested by MPC. This is marked by the transition from positive to negative force in any form. Since MPC does not receive information about the position and orientation of THR motors, this leads to the fact that the ship is not provided with the necessary propulsion power for a short time, which, in turn, leads to a time delay between τ_c^d and τc related to the rotation time of THR motors.

From the point of view of solving the general problem of improving energy efficiency, the settings of MPC controller in this case are quite drastic. In order to compensate for the non-deterministic effect on the ship model at a speed of about 2 m/s, the task signal borders on the cases where the linear damping dominates the nonlinear effects. Overshooting the task would be smaller or even completely eliminated if it was possible, for example, to increase the value of the elements of the weight matrices $Q\nu$ in the dynamic models of the ship, which would lead to a decrease in speed. This would cause the module to move more slowly, so the delay in the force would not be as significant. However, the control law limitation will still exist due to the inability to model rotational delay in MPC. A test case and setting were chosen to reveal this. Furthermore, from an implementation point of view, the control system should be minimally dependent on setup due to the limited time for commissioning on a real vessel. One way to solve the problem of energy conservation is to limit the speed of the task τ_c^d to such a low degree that it takes into account the delay that coincides with the rotation time of THR motors. However, this significantly reduces the usable performance of THR motor control system.

2. Testing of thruster configurations revealed performance degradation of separate MCSs due to the need to generate forces in more than one degree of freedom at the same time, for example, for thrust and yaw tasks. This turned out to be a consequence of MPC not modeling any relationship between forces and moments. This shortcoming is due to the chosen configuration of location of the THR motors, which does not allow the MPC to independently generate forces and moments in all degrees of freedom, or to instantly create a force in any direction. In fact, the dynamic MPC model simulates a ship equipped with a sufficient number of THR actuators, which allows it to independently generate force and moment in all degrees of freedom. However, this can lead to significant costs, especially for vessels that do not normally need to use all THR drives. The results of the first test trial for the separated MCS control mode confirmed the hypothesis of the impact on the energy efficiency of the predictive control system using a high-level controller. However, the uncertainty of certain boundary conditions for some THR locations requires leaving the system distributed. Measuring the parameters of distributed subsystems and the corresponding conditions for achieving a certain level of adequacy in terms of maintaining energy efficiency requires ongoing reconfiguration of the system, which is not always possible. According to the results of the tests, it turned out that the parameterization of THR in terms of determining the input control signals is not a task of either optimal or predictive control. Coordination of input-output signals between distributed subsystems should take place at the stage of development of elements of each separate subsystem with subsequent settings of both individual MPC controllers and the MCS system as a whole. The fact that there is some overshoot for the decoupled motion control system in terms of the given ship position indicates more of an attempt by the system to be energy efficient than a constraint on optimality. The same is confirmed by the improvement of the indicators of compliance of the resulting signals with the given ones in the range of 5–10 %, which indicates the improvement of the adjustable properties of predictive control system from the point of view of its optimality for different location of THRs.

Conflicts of interest

The authors declare that they have no conflicts of interest in relation to the current researching, including financial, personal, authorship, or any other, that could affect the researching, as well as the results reported in this paper.

Funding

Research was carried out within the framework of projects in scientific fundamental and applied research and scientific and technical (experimental) developments, financed by the Ministry of Education and Science of Ukraine:

– scientific research work "Energy installation, propulsion system, and control system over an autonomous dual-purpose floating device" (State registration number 0120U102577;

– research work "Energy-efficient dual-purpose vessel positioning system" (State registration number 0119U001651).

Data availability

The manuscript has associated data in the data warehouse.

Use of artificial intelligence

The authors confirm that they did not use artificial intelligence technologies when creating the current work.

References

1. Budashko, V. (2017). Formalization of design for physical model of the azimuth thruster with two degrees of freedom by computational fluid dynamics methods. Eastern-European Journal of Enterprise Technologies, 3 (7 (87)), 40–49. https://doi.org/10.15587/1729-4061.2017.101298
2. Fossen, T. I. (2021). Handbook of Marine Craft Hydrodynamics and Motion Control. Wiley. https://doi.org/10.1002/9781119575016
3. van Goor, P., Hamel, T., Mahony, R. (2023). Constructive Equivariant Observer Design for Inertial Navigation. IFAC-PapersOnLine, 56 (2), 2494–2499. https://doi.org/10.1016/j.ifacol.2023.10.1229
4. Maidana, R. G., Kristensen, S. D., Utne, I. B., Sørensen, A. J. (2023). Risk-based path planning for preventing collisions and groundings of maritime autonomous surface ships. Ocean Engineering, 290, 116417. https://doi.org/10.1016/j.oceaneng.2023.116417
5. Bekker, J. R., Dou, S. X. (2002). A Packaged System Approach to DP Vessel Conversion. Dynamic Positioning Conference. Available at: http://dynamic-positioning.com/proceedings/dp2002/workboats_packaged_system.pdf
6. Cozijn, H., Hallmann, R., Koop, A. (2010). Analysis of the velocities in the wake of an azimuthing thruster, using PIV measurements and CFD calculations. Dynamic positioning conference: thrusters session. Available at: https://dynamic-positioning.com/proceedings/dp2010/thrusters_cozijn.pdf
7. Furmanik, M., Konvičnə, D., Rafajdus, P. (2023). Low-Speed Sensorless Control for Six-Phase PMSM Based on Magnetic Anisotropy. Transportation Research Procedia, 74, 892–899. https://doi.org/10.1016/j.trpro.2023.11.222
8. Hemalatha, N., Venkatesan, S., Kannan, R., Kannan, S., Bhuvanesh, A., Kamaraja, A. S. (2024). Sensorless speed and position control of permanent magnet BLDC motor using particle swarm optimization and ANFIS. Measurement: Sensors, 31, 100960. https://doi.org/10.1016/j.measen.2023.100960
9. Sun, L. (2022). Low speed sensorless control method of brushless DC motor based on pulse high frequency voltage injection. Alexandria Engineering Journal, 61(8), 6457–6463. https://doi.org/10.1016/j.aej.2021.12.005
10. Budashko, V., Sandler, A., Khniunin, S. (2023). Improving the method of linear-quadratic control over a physical model of vessel with azimuthal thrusters. Eastern-European Journal of Enterprise Technologies, 1 (2 (121)), 49–71. https://doi.org/10.15587/1729-4061.2023.273934
11. de A. Fernandes, D., Sorensen, A. J., Donha, D. C. (2013). Trajectory Tracking Motion Control System for Observation Class ROVs. IFAC Proceedings Volumes, 46 (33), 251–256. https://doi.org/10.3182/20130918-4-jp-3022.00025
12. Houska, B., Ferreau, H. J., Diehl, M. (2011). ACADO toolkit – An open-source framework for automatic control and dynamic optimization. Optimal Control Applications and Methods, 32 (3), 298–312. https://doi.org/10.1002/oca.939
13. Johansen, T. A., Fossen, T. I. (2013). Control allocation – A survey. Automatica, 49 (5), 1087–1103. https://doi.org/10.1016/j.automatica.2013.01.035
14. Yari, E., Ghassemi, H. (2016). Hydrodynamic analysis of the surface-piercing propeller in unsteady open water condition using boundary element method. International Journal of Naval Architecture and Ocean Engineering, 8 (1), 22–37. https://doi.org/10.1016/j.ijnaoe.2015.09.002
15. Budashko, V., Sandler, A., Shevchenko, V. (2022). Diagnosis of the Technical Condition of High-tech Complexes by Probabilistic Methods. TransNav, the International Journal on Marine Navigation and Safety of Sea Transportation, 16 (1), 105–111. https://doi.org/10.12716/1001.16.01.11
16. Glad, T., Ljung, L. (2018). Control Theory. CRC Press. https://doi.org/10.1201/9781315274737
17. Budashko, V. (2020). Thrusters Physical Model Formalization with regard to Situational and Identification Factors of Motion Modes. 2020 International Conference on Electrical, Communication, and Computer Engineering (ICECCE), 10, 1–6. https://doi.org/10.1109/icecce49384.2020.9179301
18. Brezina, A., Thomas, S. (2013). Measurement of Static and Dynamic Performance Characteristics of Electric Propulsion Systems. 51st AIAA Aerospace Sciences Meeting Including the New Horizons Forum and Aerospace Exposition. https://doi.org/10.2514/6.2013-500
19. Bucknall, R. W. G., Ciaramella, K. M. (2010). On the Conceptual Design and Performance of a Matrix Converter for Marine Electric Propulsion. IEEE Transactions on Power Electronics, 25 (6), 1497–1508. https://doi.org/10.1109/tpel.2009.2037961
20. Zhong, Y., Yu, C., Bai, Y., Zeng, Z., Lian, L. (2024). Diving dynamics identification and motion prediction for marine crafts using field data. Journal of Ocean Engineering and Science, 9 (4), 391–400. https://doi.org/10.1016/j.joes.2023.12.001
21. Abdessameud, A., Polushin, I. G., Tayebi, A. (2015). Motion coordination of thrust-propelled underactuated vehicles with intermittent and delayed communications. Systems & Control Letters, 79, 15–22. https://doi.org/10.1016/j.sysconle.2015.02.006
22. Babadi, M. K., Ghassemi, H. (2013). Effect of hull form coefficients on the vessel sea-keeping performance. Journal of Marine Science and Technology. – 2013. – 11 p. https://doi.org/10.6119/JMST-013-0117-2
23. Budashko, V., Sandler, A., Shevchenko, V. (2022). Optimization of the control system for an electric power system operating on a constant-power hyperbole. Eastern-European Journal of Enterprise Technologies, 1 (8 (115)), 6–17. https://doi.org/10.15587/1729-4061.2022.252172
24. Carrera, A., Palomeras, N., Hurtys, N., Kormushev, P., Carreras, M. (2015). Cognitive system for autonomous underwater intervention. Pattern Recognition Letters, 67, 91–99. https://doi.org/10.1016/j.patrec.2015.06.010

25. Budashko, V., Golikov, V. (2017). Theoretical-applied aspects of the composition of regression models for combined propulsion complexes based on data of experimental research. Eastern-European Journal of Enterprise Technologies, 4 (3 (88)), 11–20. https://doi.org/10.15587/1729-4061.2017.107244
26. Myrhorod, V., Hvozdeva, I., Budashko, V. (2020). Multi-parameter Diagnostic Model of the Technical Conditions Changes of Ship Diesel Generator Sets. 2020 IEEE Problems of Automated Electrodrive. Theory and Practice (PAEP), 1895, 1–4. https://doi.org/10.1109/paep49887.2020.9240905
27. Budashko, V., Shevchenko, V. (2021). The synthesis of control system to synchronize ship generator assemblies. Eastern-European Journal of Enterprise Technologies, 1 (2 (109)), 45–63. https://doi.org/10.15587/1729-4061.2021.225517
28. Budashko, V., Shevchenko, V. (2021). Solving a task of coordinated control over a ship automated electric power system under a changing load. Eastern-European Journal of Enterprise Technologies, 2 (2 (110)), 54–70. https://doi.org/10.15587/1729-4061.2021.229033
29. Sandler, A., Budashko, V. (2022). Improving tools for diagnosing technical condition of ship electric power installations. Eastern-European Journal of Enterprise Technologies, 5 (5 (119)), 25–33. https://doi.org/10.15587/1729-4061.2022.266267
30. Sandler, A., Budashko, V., Khniunin, S., Bogach, V. (2023). Improving the mathematical model of a fiber-optic inclinometer for vibration diagnostics of elements in the propulsion system with sliding bearings. Eastern-European Journal of Enterprise Technologies, 5 (5 (125)), 24–31. https://doi.org/10.15587/1729-4061.2023.289773